

THERMAL DEAMINATION KINETICS OF TRIS(ETHYLENE-DIAMINE)NICKEL(II) SULPHATE IN THE SOLID-STATE

K. S. Rejitha and S. Mathew*

School of Chemical Sciences, Mahatma Gandhi University, P.D. Hills, Kottayam 686 560, Kerala, India

Thermogravimetric techniques have been used to study the kinetics of thermal deamination of tris(ethylenediamine)nickel(II) sulphate. The complex was synthesized and characterized by various chemical and spectral techniques. Thermal decomposition studies were carried at different heating rates (5, 10, 15 and 20°C min⁻¹) in dynamic air. The complex undergoes a four-stage decomposition pattern. The stages are not well resolved. Decomposition path can be interpreted as a two-stage deamination, and a two-stage decomposition. Reaction products at each stage were separated and identified by means of IR and XRD. The morphology of the complex and the residue were studied by means of SEM. Final residue of the decomposition was found to be crystalline NiO.

The deamination kinetics was studied using model-free isoconversional methods viz., Friedman, Flynn–Wall–Ozawa (FWO) and Kissinger–Akahira–Sunose (KAS) methods. It is observed that the activation energy varies with the extent of conversion; indicating the complex nature of the deamination reaction.

Keywords: deamination, kinetics, nickel oxide, thermal decomposition

Introduction

Thermal decomposition studies of transition metal ammine complexes especially those of Cu, Ni and Co have been extensively studied over years. However, thermal analyses of certain complexes have received renewed interest because of the formation of certain intermediates, which are otherwise difficult to synthesize [1–6]. Transition metal ammine complexes can be used as template for zeolite synthesis as they carry high positive charge density for interaction with the anionic silicate species and offer novel architecture which is not common with classic quaternary ammonium templates [7]. Obviously, thermal decomposition studies have immense application in materials synthesis where the knowledge of the decomposition temperature of the precursor is a pre-requisite for the synthesis of nanosized metal oxide and metals under appropriate conditions. In fact, now thermal decomposition technique is an important route for the synthesis of nano-materials [8–10]. In this context it is interesting to investigate the thermal decomposition behaviour of tris(ethylenediamine)nickel(II) sulphate in the solid-state. The thermolysis of nickel compounds always lead to the formation of NiO as the final product. Li *et al.* synthesized nano-sized NiO using pyrolysis of nickeldimethylglyoximate rods [11]. Present work aims to explore the thermal behaviour of tris(ethylenediamine)nickel(II) sulphate and to evaluate the kinetic scheme of thermal deamination reaction.

The kinetic analyses of the deamination stages were done using model-free isoconversional methods viz., Friedman [12], Flynn–Wall–Ozawa (FWO) [13, 14], Kissinger–Akahira–Sunose (KAS) [15, 16] methods. A series of activation energy (*E*) were determined for the deamination stage.

Experimental

Preparation of the complex

The complex, Ni(en)₃SO₄ was synthesized as per the procedure in [17]. Stoichiometric amount of ethylenediamine was added to nickel sulphate solution with stirring and cooled in ice bath. The complex was precipitated out by adding ethanol. The isolated complex was washed with ethanol and then with ether and dried over vacuum. The resulting complex was characterized by various spectral and chemical means. The nickel content in the complex was determined by gravimetry [18]. Nickel is precipitated by the addition of ethanolic solution of dimethylglyoxime to a hot faintly acidic solution of the nickel complex, and then adding a slight excess of aqueous ammonia solution. The precipitate is washed with cold water and then weighed as nickel dimethylglyoximate after drying at 110–120°C.

Instrumentation

Thermogravimetric analyses were carried out using Shimadzu DTG-60 instrument connected to TA60 on-

* Author for correspondence: sureshmathews@sancharnet.in

line analyser. The samples were loaded in a platinum crucible and the mass was kept constant around 12 ± 0.6 mg. The experiment was carried out in dynamic air. The heating rates employed were 5, 10, 15, $20^{\circ}\text{C min}^{-1}$. IR spectra were recorded on a Shimadzu 2600 FTIR instrument using KBr pellet technique. CHNS analyses were carried out on a Vario Elementar III analyzer. The X-ray powder patterns were recorded using Bruker D8 Advance diffractometer using CuK_{α} radiation ($\lambda=1.542$ Å). The particle size can be calculated using Scherrer equation [19],

$$t=0.9\lambda/\beta\cos\theta \quad (1)$$

where t is the thickness of the particle, λ is the wavelength, β is full width at half maximum (FWHM), θ is the corresponding angle.

SEM studies were carried out on a JEOL JSM 6390 instrument. The samples were uniformly spread on a carbon tape and coated with platinum.

Kinetic studies

Solid-state reaction often follows the basic kinetic equation

$$\frac{d\alpha}{dt}=A\exp\frac{-E}{RT}f(\alpha) \quad (2)$$

where A is the pre-exponential factor, E is the activation energy, R is the gas constant and T is the temperature, $f(\alpha)$ is the kinetic model function. For a non-isothermal reaction Eq. (2) can be written as

$$\frac{d\alpha}{f(\alpha)}=\frac{A}{\phi}\exp\frac{-E}{RT}dT \quad (3)$$

where ϕ is the heating rate employed and

$$\phi=\frac{dT}{dt} \quad (4)$$

Isoconversional method has the advantage that it allows the estimation of kinetic parameters without choosing a reaction model. Friedman, FWO and KAS equations represent isoconversional methods, and are frequently employed to study the kinetics. These methods yield activation energy (E) as a function of extent of conversion (α). From the dependence of E on the extent of conversion, we can infer the multi-step nature of solid-state reactions. Besides, it reveals some mechanistic conclusions.

In order to study the kinetics using the model-free methods, several TG measurements were carried out at different heating rates.

Friedman equation is

$$\ln\frac{d\alpha}{dt}=\ln[Af(\alpha)]-\frac{E}{RT} \quad (5)$$

where $d\alpha/dt$ is the rate of conversion, and $f(\alpha)$ is the mechanism function.

Flynn–Wall–Ozawa equation is as follows

$$\ln\phi=\ln\frac{AE}{R}-\ln g(\alpha)-5.3305-1.052\frac{E}{RT} \quad (6)$$

where ϕ is the heating rate, α is the degree of conversion, $g(\alpha)$ is the mechanism function, E is the activation energy, A is the pre-exponential factor, and R is the gas constant.

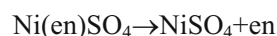
Kissinger–Akahira–Sunose (KAS) equation is

$$\ln\left(\frac{\phi}{T^2}\right)=\ln\frac{A}{Eg(\alpha)}-\frac{Ea}{RT} \quad (7)$$

From the above Eqs (5)–(7) it is seen that the plots of $\ln\phi$ vs. $1/T$, $\ln(d\alpha/dt)$ vs. $1/T$ and $\ln(\phi/T^2)$ vs. $1/T$ would give straight lines with slopes $-1.052E/R$, $-E/R$ and $-E/R$, respectively for the FWO, Friedman and KAS equations. The slope of the straight lines is directly proportional to the activation energy.

Results and discussion

The results of the elemental analysis are summarized in Table 1. The decomposition patterns at different heating rates are given in Fig. 1. The various stages of decomposition are as follows



The shapes of the TG curves remain unchanged while there is a noticeable increase in the temperature of inception (T_i), final temperature (T_f) and the DTG peak temperature (T_s) with increase in the heating

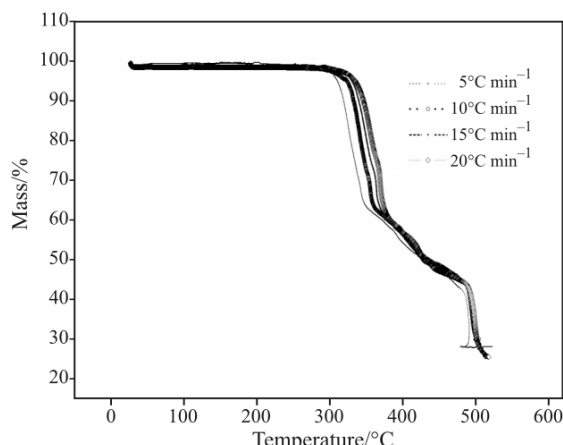


Fig. 1 TG plots at different heating rates

Table 1 Elemental analysis data

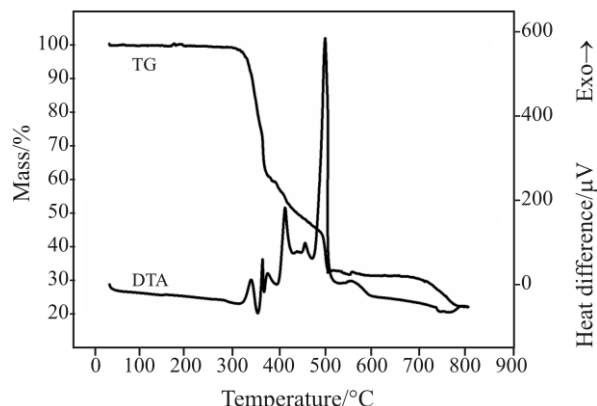
Ni/%	C/%	H/%	N/%	S/%
obsd. (calcd.)	obsd. (calcd.)	obsd. (calcd.)	obsd. (calcd.)	obsd. (calcd.)
17.52 (17.49)	21.51 (21.52)	7.22 (7.16)	25.08 (24.98)	9.57 (9.55)

rates. The decomposition starts at low temperature for a slow heating rate and ends at low temperature. It was observed that the reaction interval ($T_f - T_i$) is increased with heating rate [20]. TG/DTA plot for the thermal decomposition at a heating rate of $10^\circ\text{C min}^{-1}$ is shown in Fig. 2.

The phenomenological data for the thermal decomposition at $10^\circ\text{C min}^{-1}$ are shown in Table 2. From the TG curve at $10^\circ\text{C min}^{-1}$, it is seen that the complex starts to loss mass at 300°C , indicating the thermal stability of the complex. This stability is due to the bidentate nature of the ligand coordinating with the metal, resulting in the formation of complex with octahedral geometry. The first stage of the decomposition of tris(ethylenediamine)nickel(II) sulphate corresponds to the loss of two molecules of ethylenediamine (36% loss) to give mono ethylenediamine complex. The mono(ethylenediamine)nickel(II) sulphate is very unstable and suddenly decomposes at 360°C . The subsequent stages are overlapping and hence not distinguishable.

Intermediate formed at 500°C was separated and identified. This stage corresponds to the partial dissociation of NiSO_4 to a mixture of NiSO_4 and NiO . This was further confirmed by IR and XRD analyses. Mass loss of 77.5% at 800°C corresponds to the formation of NiO . During the temperature range (500 - 800°C) an almost continuous process was observed for which well defined DTA could not be obtained.

Thermal decomposition studies of tris(ethylenediamine)nickel(II) sulphate have been reported in the literature [1, 21]. However both studies pertain to the

**Fig. 2** TG/DTA plot at heating rate $10^\circ\text{C min}^{-1}$

decomposition carried at a single heating rate contrary to our investigation. The obtained decomposition profile differs from those of reported earlier. Wendlandt and George [1] reported a single stage decomposition pattern for the complex. The DTA contained three endotherms. While Mitra *et al.* [21] reported two stage decomposition pattern for tris(ethylenediamine)nickel(II) sulphate. The DTA pattern contained two endotherms and exotherms. Independent pyrolysis was carried out in a muffle furnace under non-isothermal conditions. Results are given in Table 2, which are in good agreement with the thermogravimetric results. The complex and the intermediates were separated and identified by means of XRD and IR. Figure 3 shows the IR spectra of the complex, intermediate at 500°C and the final residue. IR spectrum of the intermediate isolated at 500°C contains the peaks corresponding to SO_4^{2-} groups. The peaks at 1110 , 980 and 610 cm^{-1} are characteristics of SO_4^{2-} group [22].

XRD powder patterns of the complex, intermediate at 500°C and the residue at 800°C are shown in Fig. 4. Structural elucidation by single crystal X-ray investigation revealed that tris(ethylenediamine)nickel(II) sulphate crystallizes in trigonal space group $p\bar{3}1c$ with unit cell dimensions $a=b=8.946$ and

Table 2 Phenomenological data for the thermal decomposition of tris(ethylenediamine)nickel(II) sulphate ($\phi 10^\circ\text{C min}^{-1}$)

Stages	Decomposition	TG results			Mass loss/%		Independent pyrolysis mass loss/%		
		$T_i/\text{°C}$	$T_f/\text{°C}$	$T_s/\text{°C}$	Theor.	Obs.	Theor.	Obs.	Residue
1	Loss of two molecules of en	300	360	350	36.5	36.3	36.5	36	$\text{Ni(en)} \text{ SO}_4$
2	Loss of one molecule of en	360	466	410	18	17.89	18	17.85	NiSO_4
3	Decomposition of NiSO_4	466	500	490					Mixture of NiSO_4 and NiO
4	Decomposition of mixture of NiSO_4 and NiO	696	786		77.7	77.5	77.7	78	NiO

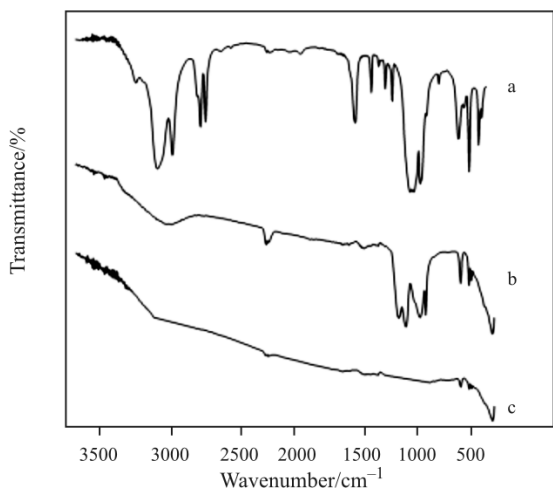


Fig. 3 IR spectra of a – $\text{Ni}(\text{en})_3\text{SO}_4$, b – mixture of NiSO_4 and NiO , c – NiO

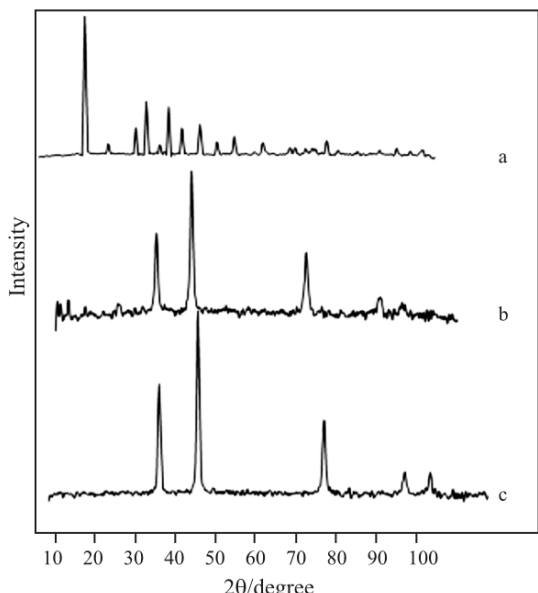


Fig. 4 XRD pattern of a – $\text{Ni}(\text{en})_3\text{SO}_4$, b – mixture of NiSO_4 and NiO , c – NiO

$c=9.634 \text{ \AA}$ [23]. The XRD peaks obtained are matching with that of JCPDS file of the complex [24]. The XRD pattern of the intermediate isolated at 500°C has (Fig. 4b) peaks of NiSO_4 and NiO . However, the majority peaks are those of NiO phase. The elemental analysis of the intermediate separated confirmed the presence of sulphur. The XRD analysis revealed that the final residue is NiO [25]. NiO has got well defined peaks with cubic symmetry. From the peak broadening value particle size of NiO was calculated using Scherrer equation. Average particle size was found to be 17.47 nm. The SEM pictures of the complex tris(ethylenediamine)nickel(II) sulphate and the residue are shown in Fig. 5. The complex has a rod like

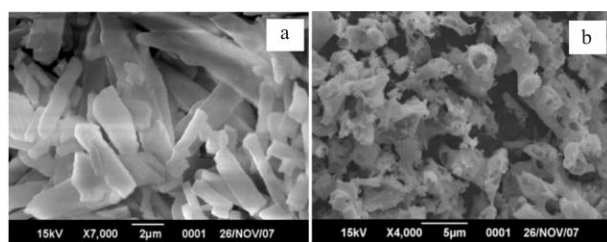


Fig. 5 SEM pictures of a – $\text{Ni}(\text{en})_3\text{SO}_4$ and b – NiO

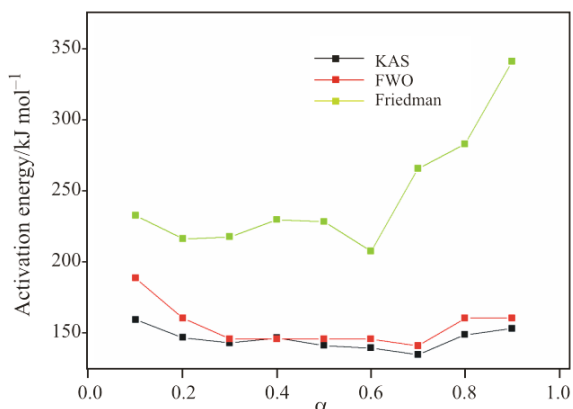


Fig. 6 Variation of activation energy with conversion (α)

appearance and NiO (residue) is found to be as hollow structure and got agglomerated.

A plot of activation energy vs. conversion function is given in Fig. 6. The kinetic parameters obtained from FWO and KAS equations are almost equal while higher values are obtained for Friedman method.

The activation energy varies with the extent of conversion. Activation energy was found to be decreasing with the extent of conversion in the range 0.05 to 0.7 and then found to be increasing. The decreasing dependence of activation energy on the conversion function can be concluded as a kinetic scheme of endothermic reversible reaction followed by an irreversible one. Increasing dependence of activation energy with conversion indicates that reaction involves parallel reaction [26–28].

References

- 1 W. W. Wendlandt and J. P. Smith, Thermal Properties of Transition Metal Ammine Complexes, Elsevier, Amsterdam 1967.
- 2 S. Mathew, C. G. R. Nair and K. N. Ninan, Thermochim. Acta, 144 (1989) 33.
- 3 C. G. R. Nair, S. Mathew and K. N. Ninan, Thermochim. Acta, 150 (1989) 63.
- 4 W. Ferenc, A. Walków-Dziewulska and B. Bocian, J. Therm. Anal. Cal., 79 (2005) 145.
- 5 N. T. Madhu, P. K. Radhakrishnan and W. Linert, J. Therm. Anal. Cal., 84 (2006) 607.

- 6 P. M. Takahashi, A. V. G. Netto, A. E. Mauro and R. C. G. Frem, *J. Therm. Anal. Cal.*, 79 (2005) 335.
- 7 J. Kecht, S. Mintova and T. Bein, *Chem. Mater.*, 19 (2007) 1203.
- 8 M. Stefanescu, O. Stefanescu, M. Stoia and C. Lazau, *J. Therm. Anal. Cal.*, 88 (2007) 27.
- 9 Y. Guo, R. Weiss, R. Boese and M. Epple, *Thermochim. Acta*, 446 (2006) 101.
- 10 P.S. Nair and G. D. Scholes, *J. Mater. Chem.*, 16 (2006) 467.
- 11 X. Li, X. Zhang, Z. Li and Y. Qian, *Solid State Commun.*, 137 (2006) 581.
- 12 H. L. Friedman, *J. Polym. Sci., Part C*, 6 (1963) 183.
- 13 J. H. Flynn and L. A. Wall, *J. Polym. Sci., Part B*, 4 (1996) 323.
- 14 T. Ozawa, *Bull. Chem. Soc. Jpn.*, 38 (1965) 1881.
- 15 H. E. Kissinger, *Anal. Chem.*, 29 (1957) 1702.
- 16 T. Akahira and T. Sunose, *Res. Rep. Chiba Inst. Technol.*, 16 (1971) 22.
- 17 E. G. Rochow, Ed., *Inorganic Synthesis*, Vol. VI, McGraw-Hill, New York 1960.
- 18 A. G. Vogel, *Text Book of Quantitative Inorganic Analysis*, Longmann, 4th Ed., 1978.
- 19 A. R. West, *Solid State Chemistry and its Applications*, 2nd Ed., John Wiley and Sons, Singapore 2003.
- 20 W. W. Wendlandt, *Thermal Methods of Analysis*, 3rd Ed., Wiley Interscience 1986.
- 21 S. Mitra, G. De and N. R. Chaudhury, *Thermochim. Acta*, 71 (1983) 107.
- 22 N. Nakamoto, *Infrared and Raman Spectra of Inorganic and Coordination Compounds*, 5th Ed., John Wiley and Sons, New York 1999.
- 23 M. Ul-Haque, C. N. Caughlan and K. Emerson, *Inorg. Chem.*, 9 (1970) 2421.
- 24 JCPDS card No: 23-1796.
- 25 JCPDS card No: 47-1049.
- 26 S. Vyazovkin and W. Linert, *Int. J. Chem. Kinet.*, 27 (1995) 73.
- 27 S. Vyazovkin, *Int. J. Chem. Kinet.*, 28 (1996) 95.
- 28 S. Vyazovkin and A. I. Lesnikovich, *Thermochim. Acta*, 165 (1990) 273.

DOI: 10.1007/s10973-007-8923-9